



Observations of volcanic SO₂ from MLS on Aura

H. C. Pumphrey¹, W. G. Read², N. J. Livesey², and K. Yang³

¹School of GeoSciences, The University of Edinburgh, Edinburgh, UK

²Jet Propulsion Laboratory, California Institute of Technology, Pasadena, CA, USA

³Department of Atmospheric and Oceanic Science, University of Maryland, College Park, MD, USA

Correspondence to: H. C. Pumphrey (hugh.pumphrey@ed.ac.uk)

Received: 29 May 2014 – Published in Atmos. Meas. Tech. Discuss.: 31 July 2014

Revised: 17 November 2014 – Accepted: 4 December 2014 – Published: 12 January 2015

Abstract. Sulfur dioxide (SO₂) is an important atmospheric constituent, particularly in the aftermath of volcanic eruptions. These events can inject large amounts of SO₂ into the lower stratosphere, where it is oxidised to form sulfate aerosols; these in turn have a significant effect on the climate. The MLS instrument on the Aura satellite has observed the SO₂ mixing ratio in the upper troposphere and lower stratosphere from August 2004 to the present, during which time a number of volcanic eruptions have significantly affected those regions of the atmosphere. We describe the MLS SO₂ data and how various volcanic events appear in the data. As the MLS SO₂ data are currently not validated we take some initial steps towards their validation. First we establish the level of internal consistency between the three spectral regions in which MLS is sensitive to SO₂. We compare SO₂ column values calculated from MLS data to total column values reported by the OMI instrument. The agreement is good (within about 1 DU) in cases where the SO₂ is clearly at altitudes above 147 hPa.

1 Introduction

Sulfur dioxide (SO₂) is an important minor constituent of the atmosphere. Natural tropospheric sources include volcanoes, while anthropogenic sources include combustion of fossil fuels and smelting of sulfur-containing metal ores. Tropospheric emission of SO₂ has a variety of detrimental effects on air quality and ecosystems; in particular it can be a major contributor to acid rain (Likens and Bormann, 1974). The high solubility of SO₂ in water which leads to acid rain means that very little of the SO₂ emitted at the surface reaches the stratosphere. Sulfur dioxide in the strato-

sphere may be produced in situ by chemical reactions involving other, less soluble, sulfur-containing molecules – mostly carbonyl sulfide (OCS) (Brühl et al., 2012). Sulfur dioxide may also reach the upper troposphere or stratosphere if it is emitted directly from the Earth's surface by a process which is sufficiently energetic to loft it to that altitude. A volcanic eruption is the only such process which has been observed to lead to enhanced SO₂ in the lower stratosphere.

Once in the stratosphere, SO₂ becomes an important component of the climate system (Robock, 2000). It is oxidised on a timescale of about a month, becoming aerosol particles which have a lifetime in the stratosphere of over a year. These particles alter the albedo of the Earth, reflecting a fraction of sunlight back into space and thereby reducing the Earth's temperature. Based on six of the largest eruptions of between 1875 and 1991, Robock and Mao (1995) show that the cooling can be on the order of 0.1 to 0.2 °C.

A variety of techniques exist for the remote sensing of atmospheric SO₂ from satellites. Nadir sounding provides good horizontal resolution but little or no vertical resolution. Both thermal emission in the infrared (IR) (Clarisse et al., 2012) and backscattered sunlight in the ultraviolet (UV) (Yang et al., 2007) can be used. Note that SO₂ layer heights may also be retrieved from hyper-spectral UV observations when the columns are sufficiently large (Yang et al., 2010). Limb-sounding instruments provide vertically resolved profiles but with limited horizontal resolution. Thermally emitted radiation in both the infrared (Höpfner et al., 2013) and microwave (Read et al., 1993) regions can be used for limb sounding.

The Microwave Limb Sounder, or MLS (Waters et al., 2006), is one of the four instruments on NASA's Aura satellite (Schoeberl et al., 2006). MLS measures the concentra-

tions of a suite of 14 chemical species in the upper troposphere and middle atmosphere. Sulfur dioxide (SO₂) is one of the species measured. The sensitivity of the measurement is not sufficient to detect the background levels of SO₂, but the enhanced levels present following a sufficiently large volcanic eruption are detected; it is these observations which we report in this paper. We describe the instrument and the measurement process in more detail in Sect. 2, give an overview of the volcanic events observed in Sect. 3, and examine three of the larger events in more detail in Sect. 4. In Sect. 5 we estimate the total mass of SO₂ injected into the stratosphere by the larger volcanic eruptions of the last decade. In Sect. 6 we make an initial attempt to validate the data.

2 Data

2.1 The MLS instrument

Aura (Schoeberl et al., 2006) was launched in July 2004, and the MLS instrument (Waters et al., 2006) has operated with little interruption from August 2004 to date. The satellite orbits at an altitude of 705 km, performing approximately 14.5 orbits per day. The MLS instrument consists of a 1.6 m parabolic dish antenna feeding heterodyne radiometers operating at 118, 190, 240 and 640 GHz. A separate small antenna feeds another radiometer operating at 2.5 THz. The output of the radiometers is analysed by banks of filters. The antenna looks forward from the Aura platform, in the plane of the orbit, and is scanned across the Earth's limb 240 times per orbit. As the orbit is inclined at 98° to the Equator, the instrument observes a latitude range from 82° S to 82° N every day. The observations are of thermal emission from the atmosphere and can therefore be made day and night. The orbit is sun-synchronous, so the observations are always made at the same two local times for a given latitude. The radiances reported by the filter banks are used as input to a software package (Livesey et al., 2006) which estimates profiles of temperature, and of the mixing ratios of the target chemical species. Most MLS estimated profiles, including SO₂, are reported on pressure levels spaced at six levels per pressure decade, a spacing of approximately 2.7 km in altitude. The estimated profiles are spaced 1.5° (167 km) apart along the orbit track. The software produces an estimate of the precision of every quantity estimated. All mixing ratios in this paper are produced by version 2 (V2) of this software package. The precisions and accuracies of these data are summarised in a data quality document (Livesey et al., 2007).

2.2 The MLS SO₂ measurement

The SO₂ molecule, like the H₂O and O₃ molecules, is a nonlinear triatomic molecule. A combination of this shape, a moderately large dipole moment (similar to that of water) and a large moment of inertia leads to a spectrum with a large number of strong lines and an even larger number of weak

ones. There are reasonably strong SO₂ lines present in the passband of all MLS radiometers. The software makes separate attempts to estimate the SO₂ mixing ratio from the 190, 240 and 640 GHz radiometers, but only the 240 GHz product is of sufficient quality for general use.

Three versions of the MLS data have been released to the public: V1.5, V2 and V3. Although V3 is an improvement on V2 in most respects, CO and SO₂ data in the upper troposphere are distinguished less well from clouds in V3 than in V2. For this reason we use the V2 data in this paper. The pressure levels on which SO₂ is reported and where significant amounts have been observed are 316, 215, 147, 100, 68 and 46 hPa. At altitudes below the 316 hPa level no retrieval is attempted. Retrieval is attempted between 316 hPa and 1 hPa; the sensitivity and vertical resolution of the retrieval become rapidly poorer at altitudes above 10 hPa. Between 215 and 10 hPa the vertical resolution is close to the spacing between the pressure levels, about 3 km, and the estimated precision is approximately 3 ppbv. Although retrieval is attempted at 315 hPa the data at this level are not recommended for general use. We present them in this paper but are cautious about drawing any conclusions from them. Further details on the data quality are given in Livesey et al. (2007).

Figure 1 shows data from a single pressure level, for all profiles on two different days. On 7 August 2008 the SO₂ mixing ratio, as observed by MLS, was very small compared to the measurement noise. The additional scatter seen in the tropics is caused by high clouds interfering with the retrieval. The standard deviation of the data is generally 2–4 times larger than the estimated precision, suggesting that there are contributions to the random error which are not accounted for in the retrieval software. On 11 August 2008 there are a collection of points with large and positive values; as we show in more detail below these points represent SO₂ emitted from the eruption of Kasatochi on 8 August 2008. Those points which are more than 7.7 standard deviations above the mean are marked in red. The mean and standard deviation used are for the unmarked points only; an iterative procedure was used to separate the marked points. The choice of 7.7 standard deviations as a cut-off is arbitrary and was chosen by trial and error in order to have only a small number of false positives while still identifying the major volcanic events. Figure 1 suggests that there are a number of points which are affected by volcanic SO₂ but which are below this threshold. The 7.7 standard deviation threshold is typically in the 50–100 ppbv range; this is about 100 times larger than the background SO₂ mixing ratio as measured by other instruments (see e.g. Höpfner et al., 2013).

Figure 1 also suggests that the daily zonal mean MLS SO₂ mixing ratio is not quite zero. Inspection of a time series (not shown) shows that it varies somewhat throughout the year. At most altitudes the annual cycle is largest at the poles, where it has an amplitude of about 2 ppbv. The data therefore have a bias which is dependent upon both time and latitude. We do not consider this feature of the data to be due to SO₂ in the

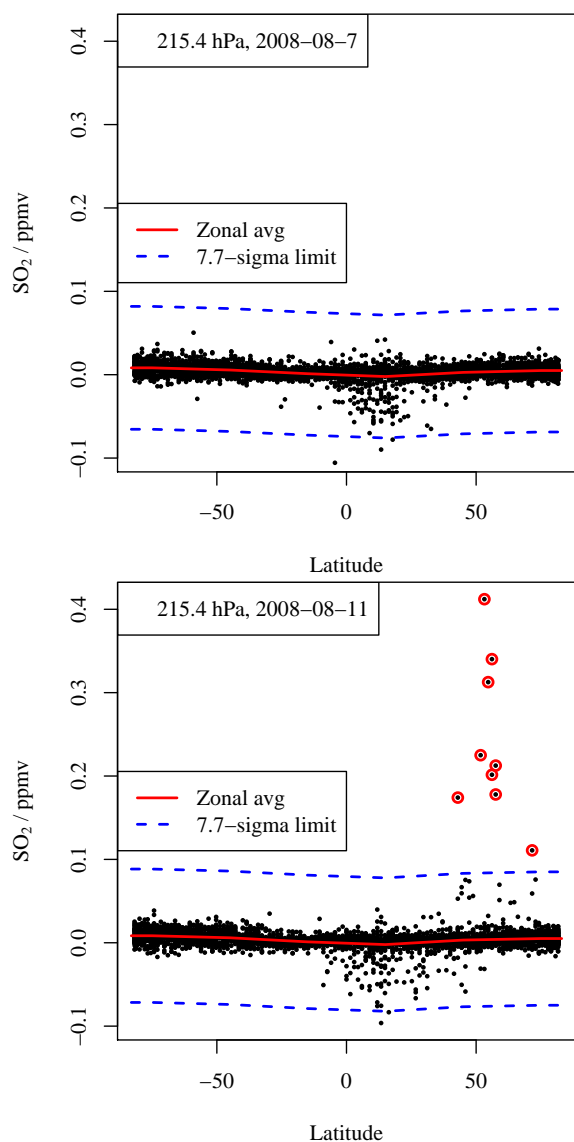


Figure 1. Scatter plot of MLS SO₂ mixing ratio against latitude for 7 and 11 August 2008 at 215 hPa. All profiles (and hence the entire 82° S to 82° N latitude range) are shown. An eruption of the volcano Kasatochi in the Aleutian Islands occurred on 8 August. Points that are more than 7.7 standard deviations above the zonal mean, and which therefore lie within the SO₂ plume caused by the eruption, are marked with red circles.

atmosphere for several reasons. Firstly, recent observations of the background SO₂ amounts by Höpfner et al. (2013) show that the true background levels are much smaller than this. Secondly, the seasonal cycles in MLS SO₂ show many features in common with the seasonal cycles in MLS measurements of ozone and nitric acid; these species have strong spectral lines in the passband of the 240 GHz radiometer. We conclude that the seasonal cycles seen in the zonal mean SO₂ data are essentially leakage of information from the O₃ and HNO₃ measurements. While the MLS data appear promis-

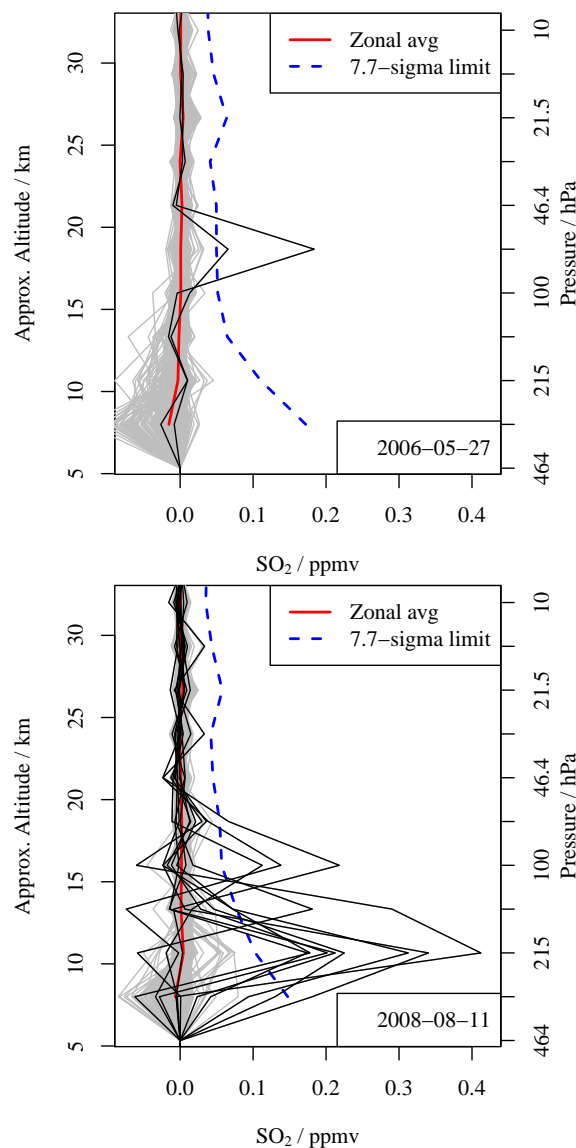


Figure 2. Profiles of SO₂ mixing ratio for a day shortly after the eruption of Soufrière hills, Montserrat, in 2006, and a day shortly after the eruption of Kasatochi in 2008. The Montserrat profiles are from 0 to 20° N; the Kasatochi profiles are from 40 to 60° N. Profiles with unusual amounts of SO₂ as defined in the text are shown in black, the other profiles in grey. The mean of the grey profiles is shown in red; the dashed blue line is 7.7 standard deviations above this mean.

ing for the study of enhanced levels of SO₂ caused by volcanoes, it is not currently possible to average them down in an attempt to study seasonal variability of the non-volcanic background or other features with amplitudes below about 2–3 ppbv.

In Fig. 2 we show some profiles for 2 days for latitude bands affected by volcanic eruptions. Points with mixing ratios greater than 7.7 standard deviations above the mean are identified as for Fig. 1, and profiles containing such a point

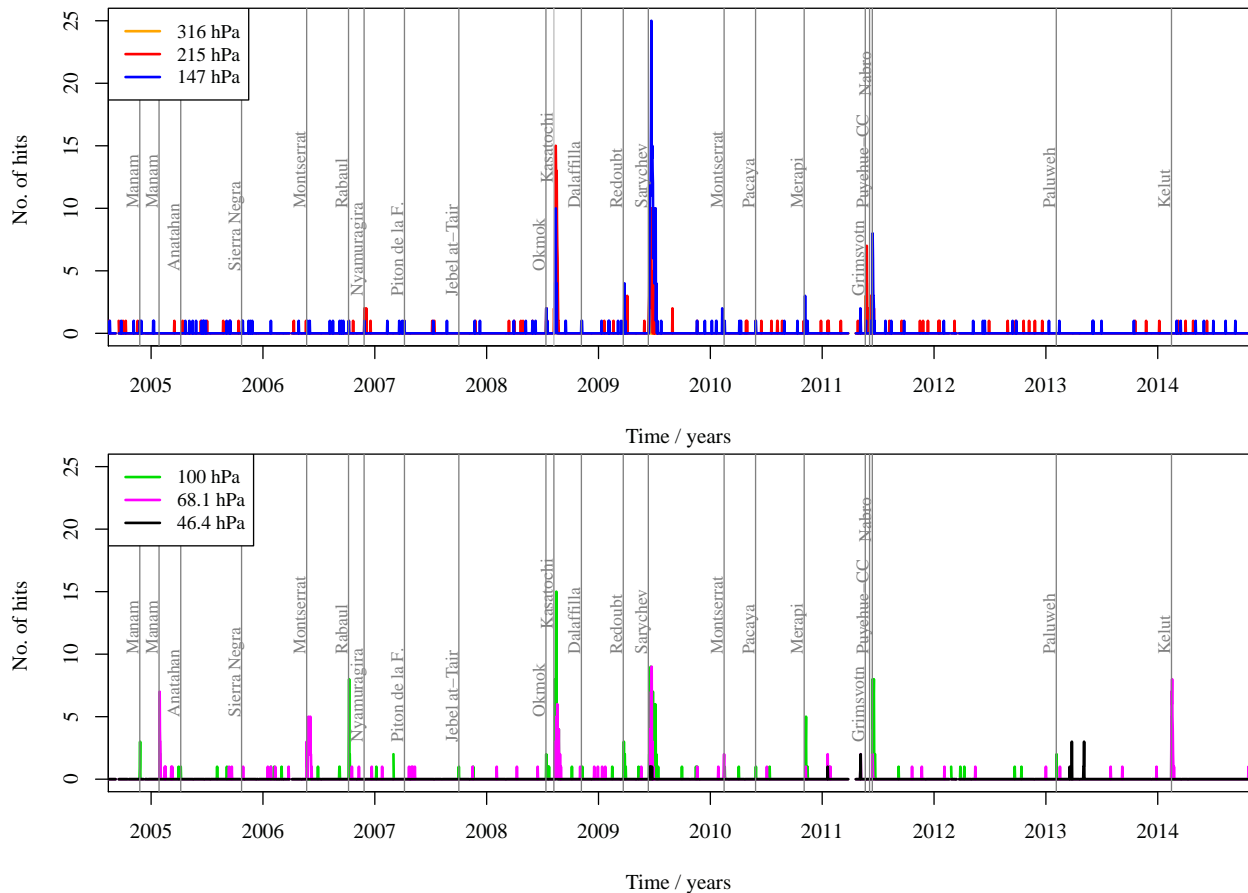


Figure 3. Number of observations of SO₂ per day for the entire mission. For the purposes of this figure an “observation” is a point in the MLS profile which is more than 7.7 standard deviations above the usual zonal mean value for that pressure and latitude.

are shown in black. The two events shown differ from each other in the vertical distribution of SO₂: in one event the SO₂ is all at the 68 hPa level, and in the other it is distributed between 68 and 316 hPa with the largest amounts at 215 hPa.

3 Event detection

We apply the detection procedure used for Figs. 1 and 2 to the entire mission; the result is shown in Fig. 3. The times of volcanic eruptions that are detected by MLS are marked on the figure. The larger events are very obvious. Some of the smaller ones are not obvious; detection was confirmed by a combination of independent reports of an eruption and co-located observations of enhanced SO₂ by the OMI instrument (also on Aura). The events marked on Fig. 3 are summarised in Table 1. Much of the information about names and locations of volcanoes, and times of eruptions, was provided by the Smithsonian Global Volcanism Program (<http://www.volcano.si.edu>). Figure 4 shows the typical mixing ratios observed in the volcanic plumes; where there is no plume the maximum value observed that day is shown. Fig-

ures 3 and 4 show a few spikes in 2011 and 2013 which on closer inspection appear to be faults or glitches in the data and do not appear to be associated with any volcanic activity.

4 Major events in more detail

In this section we examine in more detail several of the volcanic eruptions shown in Fig. 3 and Table 1.

4.1 Sarychev, June 2009

The Sarychev Peak volcano is located in the Russian Kuril island chain, between Japan and the Kamchatka Peninsula. A major eruption of the volcano occurred between 11 and 16 June 2009; the eruption is described by Rybin et al. (2011) and a detailed chronology of the explosion is given by Matoza et al. (2011). The most energetic phases of the eruption were between 12 June and 16 June. We show the time series of MLS observations of elevated SO₂ in Fig. 5 and a map of the locations of these observations in Fig. 6.

Figure 5 is produced in the same manner as Fig. 3. Note that the greatest number of observations occurs at the 147 hPa

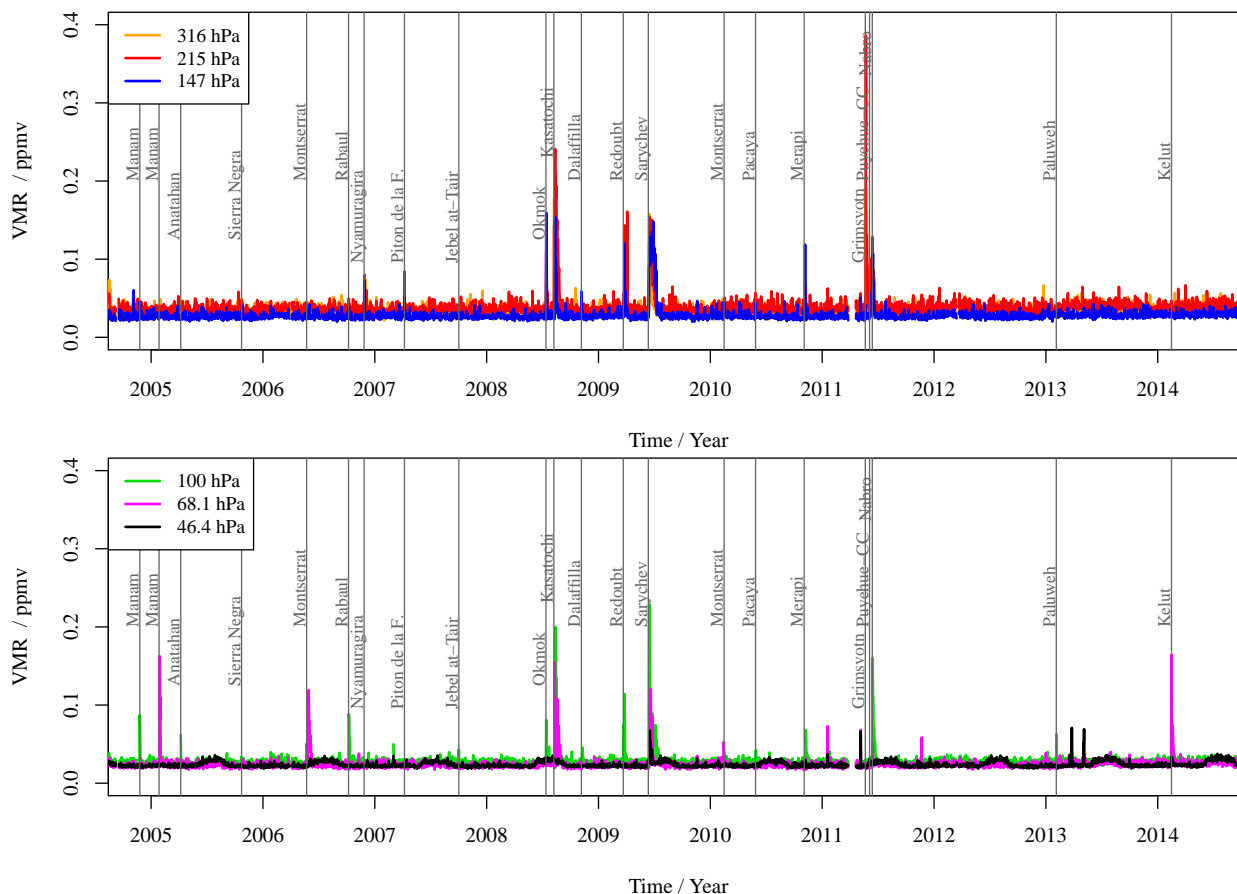


Figure 4. Average SO₂ mixing ratio for “observations” of SO₂ as defined in Fig. 3. Where there are insufficient observations, the three highest mixing ratios observed that day are used instead. This choice means that there is little artificially induced difference in the plotted data between eruption and non-eruption periods. The data plotted when there is no volcanic SO₂ observed are not typical values or daily average values either for the MLS data or for the real background SO₂.

level, but that the first observations (days 164 and 165; 13 and 14 June) are at 215 hPa. Figure 6 suggests that most of the SO₂ travelled eastwards away from the volcano, curving northwards over Canada and Alaska and dividing into two parts: one of which travelled westwards to disperse over eastern Russia, the other of which travelled eastwards across northern Canada and Greenland. A portion of the SO₂ travelled westwards away from the volcano; closer inspection suggests that this is the SO₂ that was emitted towards the end of the eruption.

4.2 Kasatochi, August 2008

The Kasatochi volcano in the Aleutian island chain erupted rather unexpectedly on 7–8 August 2008. The eruption is described by Waythomas et al. (2010) and the evolution of the SO₂ plume as observed by OMI is described by Krotkov et al. (2010).

We show the time series of MLS observations of elevated SO₂ in Fig. 7 and a map of the locations of these observations

in Fig. 8. The SO₂ plume appears to be at a slightly lower altitude than that from Sarychev; there are no detections at 46 hPa and the largest number occurs at 215 hPa rather than 146 hPa. All of the observations are to the east of the volcano; the upper level winds were presumably westerly at all altitudes at which MLS observed any volcanic SO₂. The plume experiences considerable wind shear once over North America; the SO₂ at 215 hPa travelling rapidly eastwards across the North Atlantic while that at 100 and 68 hPa remains over North America. The observations persist for a longer time at these three levels than at the intervening 147 hPa level.

4.3 Montserrat, May 2006

The Soufrière Hills volcano on the island of Montserrat in the West Indies underwent a long phase of eruptive activity between 1995 and 2010. The eruption was characterised by the repeated growth and collapse of lava domes (see Wadge et al., 2014, Loughlin et al., 2010, and references therein). Most of this activity had little impact on regions of the at-

Table 1. Table summarising MLS observations of SO₂ during various volcanic eruptions. The eruptions are sorted roughly in order of impact. For the purposes of this table an “observation” is a point in the MLS profile which is more than 7.7 standard deviations above the usual zonal mean value for that pressure and latitude.

Volcano	Location long/lat	Date of first observation	Days observed	Total no. of observations	Highest volume mixing ratio (in ppmv)
Sarychev, Kuril Islands	153.2° W, 48.1° N	14 Jun 2009	31	455	0.55 at 100 hPa
Kasatochi, Aleutian Islands	175.5° W, 52.2° N	8 Aug 2008	23	268	0.46 at 215 hPa
Soufrière Hills, Montserrat	62.2° W, 16.7° N	23 May 2006	17	39	0.18 at 68 hPa
Nabro, Eritrea	41.7° E, 13.4° N	14 Jun 2011	9	73	0.29 at 100 hPa
Kelut, Java	112.3° E, 7.93° S	14 Feb 2014	7	48	0.4 at 68 hPa
Grímsvötn, Iceland	17.3° W, 64.4° N	22 May 2011	8	30	0.5 at 215 hPa
Redoubt, Alaska	152.7° W, 60.5° N	23 Mar 2009	13	25	0.2 at 147 hPa
Okmok, Aleutian Islands	168.1° W, 53.4° N	13 Jul 2008	10	16	0.34 at 147 hPa
Manam, Papua New Guinea	145.0° E, 4.1° S	28 Jan 2005	4	22	0.28 at 68 hPa
Rabaul (Tavurvur), New Britain	152.2° E, 4.3° S	8 Oct 2006	4	18	0.16 at 100 hPa
Nyamuragira, Dem. Rep. Congo	29.2° E, 1.4° S	28 Nov 2006	7	7	0.15 at 147 hPa
Manam, Papua New Guinea	145.0° E, 4.1° S	24 Nov 2004	6	7	0.19 at 100 hPa
Puyehue-Cordón Caulle, Chile	72.1° W, 40.6° S	5 Jun 2011	3	6	0.15 at 215 hPa
Dalaffilla (a.k.a. Gabuli), Ethiopia	40.55° E, 13.8° N	5 Nov 2008	4	4	0.1 at 147 hPa
Soufrière Hills, Montserrat	62.2° W, 16.7° N	13 Feb 2010	2	3	0.087 at 68 hPa
Merapi, Indonesia	110.4° E, 7.5° S	6 Nov 2010	4	7	0.18 at 147 hPa
Pacaya, Guatemala	90.6° W, 14.4° N	27 May 2010	2	4	0.086 at 215 hPa
Piton de la Fournaise, Réunion	55.7° E, 21.2° S	7 Apr 2007	1	2	0.13 at 215 hPa
Paluweh, Indonesia	121.7° E, 8.3° S	4 Feb 2013	1	2	0.11 at 100 hPa
Anatahan, Mariana Islands	145.7° E, 16.4° N	7 Apr 2005	1	1	0.12 at 100 hPa
Sierra Negra, Galápagos Islands	91.2° W, 0.8° S	25 Oct 2005	1	1	0.048 at 147 hPa
Jabal al-Tair, Yemen	41.8° E, 15.6° N	2 Oct 2007	1	1	0.06 at 100 hPa

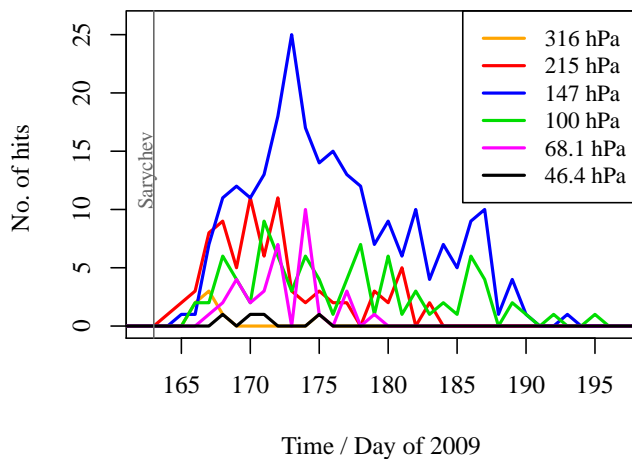


Figure 5. Number of observations of volcanic SO₂ in the days following the eruption of Sarychev. An observation is defined in the same way as in Fig. 3 and Table 1. The eruption is marked as occurring on day 163 (12 June 2009).

mosphere observable by MLS; the main exception was the dome collapse on 20 May 2006. The collapse is described by Loughlin et al. (2010) and the SO₂ release by Carn and Prata (2010) and by Prata et al. (2007).

We show the time series of MLS observations of elevated SO₂ in Fig. 9 and a map of the locations of these observations in Fig. 10. Note that the SO₂ is confined to a narrow layer,

affecting only the 68 hPa level in the MLS data. This is in agreement with the modelling results in Prata et al. (2007), which show the SO₂ forming a layer centred at a height of 20 km and full width at half maximum of 2 km. It is some days after the eruption before MLS observes any volcanic SO₂. Inspection of data from the OMI instrument, which has a higher horizontal resolution, shows that the plume was of a small size and fell between the MLS orbits between 20 May and 22 May.

5 Total SO₂ burden

We calculated the total mass of SO₂ in a suitable latitude region for each major eruption. To do this, we first calculated daily zonal means of mixing ratio. These were then integrated vertically as in Sect. 6.2.1 to give zonal mean column amounts. Finally, the column amounts are weighted by area and summed for a suitable range of latitudes. Both the latitude range and the highest pressure used in the vertical integration are chosen separately for each eruption in order to encompass all of the profiles and levels showing enhanced SO₂ from that eruption.

The results are in most cases dominated by the spurious seasonal cycle described in Sect. 2.2. As this varies smoothly in time we can remove it by fitting annual and semi-annual sinusoidal cycles to the data for the time unaffected by the eruption; a typical example is shown in Fig. 11.

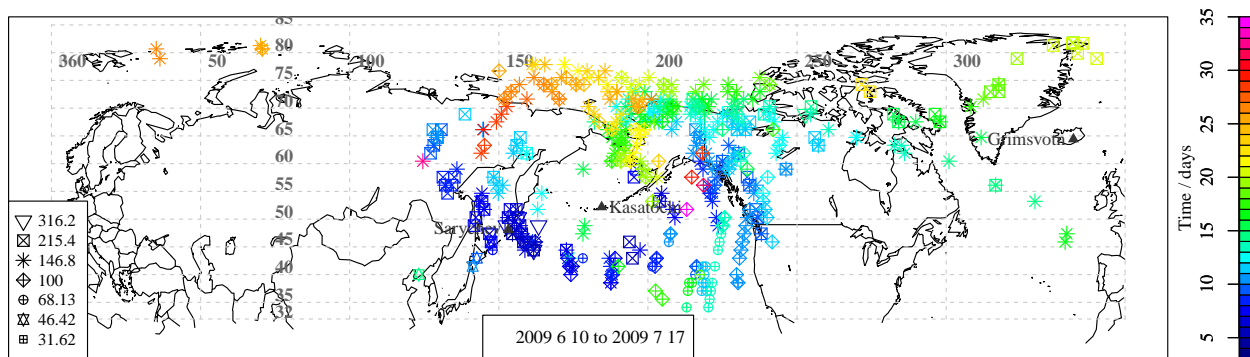


Figure 6. Locations where unusual levels of SO₂ were recorded in the days following the eruption of Sarychev which began on 11 June 2009. Colours represent time in days; day 1 is 10 June 2009. A different symbol is used for each of the MLS pressure levels.

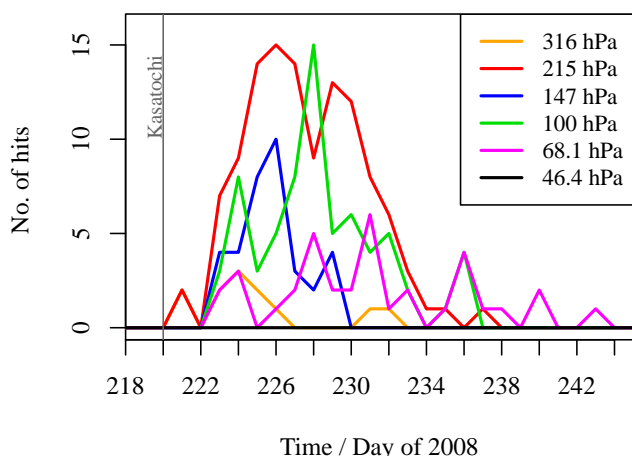


Figure 7. As Fig. 5 but for the eruption of Kasatochi in 2008 which began on 7 August 2008 (day 220).

The excess mass, M_t , above the spurious background can be adequately fitted as a function of time, t , by a decaying exponential:

$$M_t = M_0 \exp\left(\frac{-(t - t_0)}{\tau}\right)$$

or, equivalently

$$\log_e M_t = \log_e M_0 - \frac{(t - t_0)}{\tau},$$

where M_0 is the total mass injected by the volcano at time t_0 , and τ is the e -folding time for the conversion of SO₂ to sulfate aerosol. An example of such a fit is shown in Fig. 11, and a summary of the largest events observed by MLS is shown in Fig. 12. Table 2 shows the two fitted parameters M_0 and τ for each of these events.

The agreement between injected mass estimates from MLS and those found in the literature is generally good. Clear discrepancies are the much larger values reported

by Clarisse et al. (2012) for Grímsvötn and Nabro. For Grímsvötn this is unsurprising as most of the SO₂ observed by MLS is at 316 and 215 hPa; it seems likely that a fraction of the plume was at rather low altitudes, where MLS would be unable to observe it. For Nabro, most of the SO₂ observed by MLS is at 100 and 147 hPa, where we would expect the MLS observations to be reasonably good. However, Nabro is at a rather low latitude, where the ability of MLS to observe at lower altitudes is more likely to be adversely affected by high levels of water vapour in the upper troposphere. A more recent paper (Clarisse et al., 2014) gives a mass of 650 Gg above 10 km for the initial phase of the eruption; this is in somewhat better agreement with the MLS estimate. It should be noted that all of the eruptions during the Aura mission to date have been small compared to the eruption of Mount Pinatubo in 1991; Read et al. (1993) give a total mass of $M_t = 17\,000$ Gg for that eruption. The e -folding time for Pinatubo was approximately 33 days, in reasonable agreement with the values in Table 2.

6 Initial validation of the MLS data

The data we have described have not been validated. They appear reasonable at a first glance in that the values are smaller than the measurement noise except shortly after the eruption of volcanoes which have been observed erupting from the ground and from other satellites. Further validation from in situ measurements is not straightforward as for most of the time, and at most places there is not sufficient SO₂ for MLS to detect. Volcanic eruptions happen with little warning so it is not usually possible to plan aircraft or balloon campaigns to coincide with them. The most tractable approach is to cross-validate the various satellite SO₂ measurements against each other. While this process can not be considered watertight, we can feel some increased confidence if several satellite measurements using different spectral ranges and observation geometries are in agreement with each other.

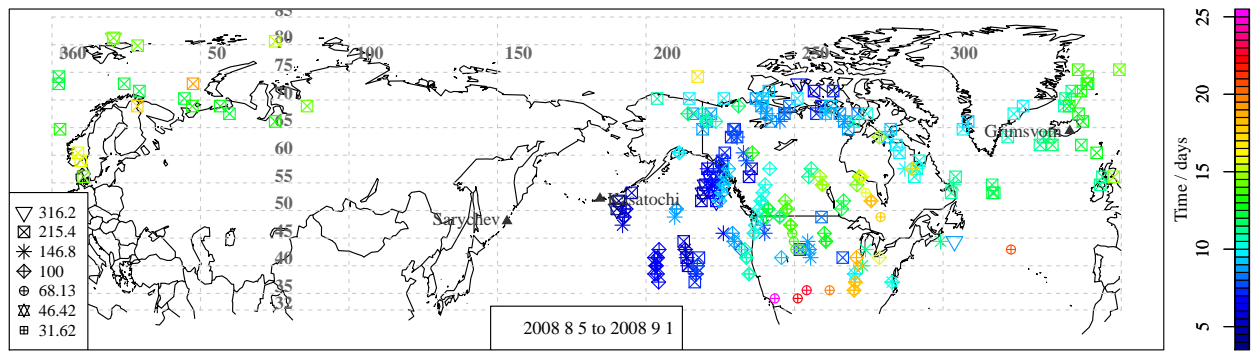


Figure 8. As Fig. 6 but for the eruption of Kasatochi which began on 7 August 2008. Colours represent time in days; day 1 is 5 August 2008.

Table 2. Total injected SO₂ mass M_0 and decay time τ for a selection of the volcanic events observed by MLS. Estimates of M_0 from other sources are shown for comparison. Krotkov et al. (2010) also give an estimate of $\tau = 9$ days for Kasatochi. For Sarychev we show two estimates for two choices of highest pressure used (p_{\max}). The 215 hPa result is more use for comparison with nadir-sounder data but is less satisfactory as it proved difficult to remove the seasonal background for this case.

Name	$p_{\max}/$ hPa	τ /days	M_0 /Gg	M_0 /Gg (from other sources)
Sarychev	147	27 ± 2	571 ± 42	
Sarychev	215	17 ± 3	1160 ± 180	1200 ± 200 (Haywood et al., 2010), 900 (Clarisse et al., 2012)
Kasatochi	215	27 ± 1	1350 ± 38	1373 (D'Amours et al., 2010), 2200 (Krotkov et al., 2010), 500 – 2500 (various references cited by Krotkov et al., 2010)
Nabro	147	20 ± 2	543 ± 45	1500 (Clarisse et al., 2012), 650 (above 10 km) (Clarisse et al., 2014)
Grímsvötn	215	17 ± 2	108 ± 11	350 – 400 (Clarisse et al., 2012)
Kelut	100	34 ± 7	144 ± 12	200 (http://so2.gsfc.nasa.gov/pix/special/2014/kelut/Kelut_summary_Feb14_2014.html)
Rabaul	100	34 ± 5	190 ± 14	230 (Carn et al., 2008)
Montserrat	68.1	22 ± 4	139 ± 24	123 – 233 (Carn and Prata, 2010)
Manam (2005)	68.1	20 ± 4	99 ± 13	

In this section we compare the standard MLS product against SO₂ estimates from the 190 and 640 GHz radiometers on the same instrument. We then compare integrated column values calculated from the MLS data to column values from the OMI instrument.

6.1 Internal consistency

As we noted in Sect. 2.2, MLS makes three partly independent estimates of SO₂: from the 190, 240 and 640 GHz radiometers. Some errors are common to all these estimates: these include errors from the temperature/pointing retrieval. Other errors, such as those from spectroscopic data, should be more-or-less uncorrelated between the three estimates. The field of view of the three radiometers is very similar, to the extent that we can consider the three measurements to be made at exactly the same time and place.

We compare the 190 and 640 GHz products against the standard 240 GHz product in Fig. 13. In order to avoid plotting an excessive number of points which are effectively zero, we consider only periods of time after a major eruption; a different colour is used for each such period. We also show only points from profiles which contain a point at some level

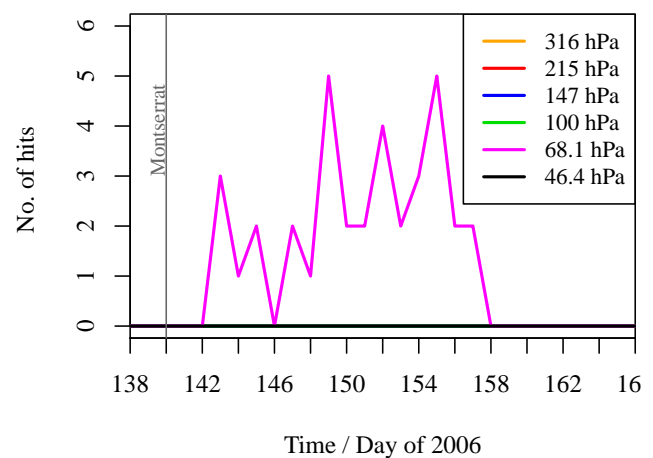


Figure 9. As Fig. 5 but for the eruption of the Soufrière hills volcano, Montserrat, on 20 May 2006.

which is more than 5.5 standard deviations above the mean for that level; this criterion is less restrictive than that used in earlier sections. For each scatter plot in Fig. 13 we fit a straight line to the data in two ways: first we assume that the

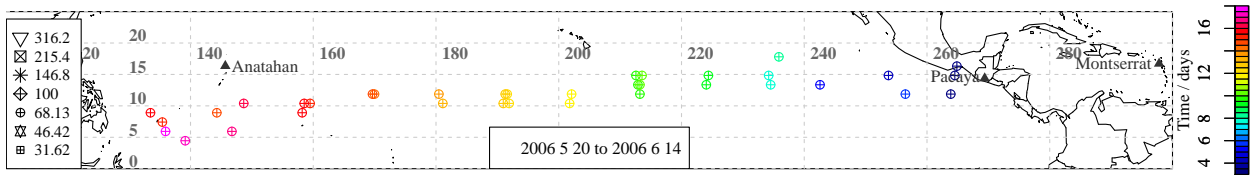


Figure 10. As Fig. 6 but for the eruption of the Soufrière hills volcano, Montserrat, on 20 May 2006. Colours represent time in days; day 1 is 20 May 2006.

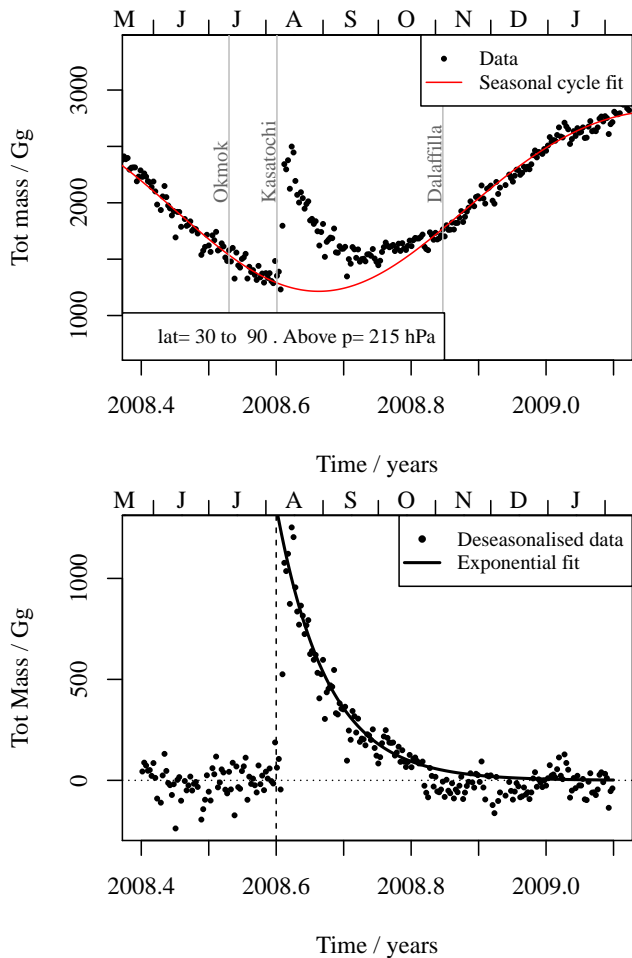


Figure 11. Isolating the volcanic SO₂ from the background value (with its spurious seasonal cycle). The example shown is for the eruption of Kasatochi.

standard product is the independent variable and that all the errors are in the 640 or 190 GHz product (dashed line $y \sim x$ in the figure). Next, we assume that all the errors are in the standard product (dot-dash line $x \sim y$). We note that in general the 640 GHz SO₂ appears to underestimate the standard 240 GHz SO₂; the slopes of the fit lines tend to be considerably less than 1. In contrast, the 190 GHz SO₂ tends to overestimate the standard product. At 46 hPa there is very little correlation between the different SO₂ products, but we note

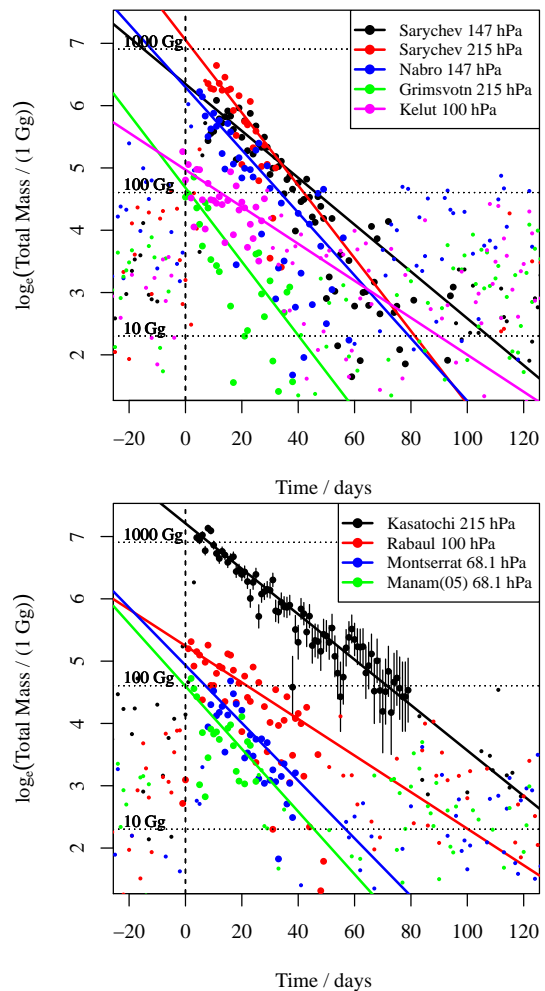


Figure 12. Mass M_t of SO₂ above background as a function of time after an eruption. The quantity plotted is $\log_e M_t$ so that the exponential decay becomes a straight line. The parameters M_0 and τ were determined by fitting the straight lines shown on this figure: the points were weighted with the inverse square of errors which are constant in M_t and hence not so in $\log(M_t)$. These errors are shown for Kasatochi. Only the large dots are used in the fit.

that the four points with mixing ratios above 0.06 ppmv lie close to the 1 : 1 line. At 68 and 100 hPa the correlation is much stronger and a larger fraction of the points are responsible for it.

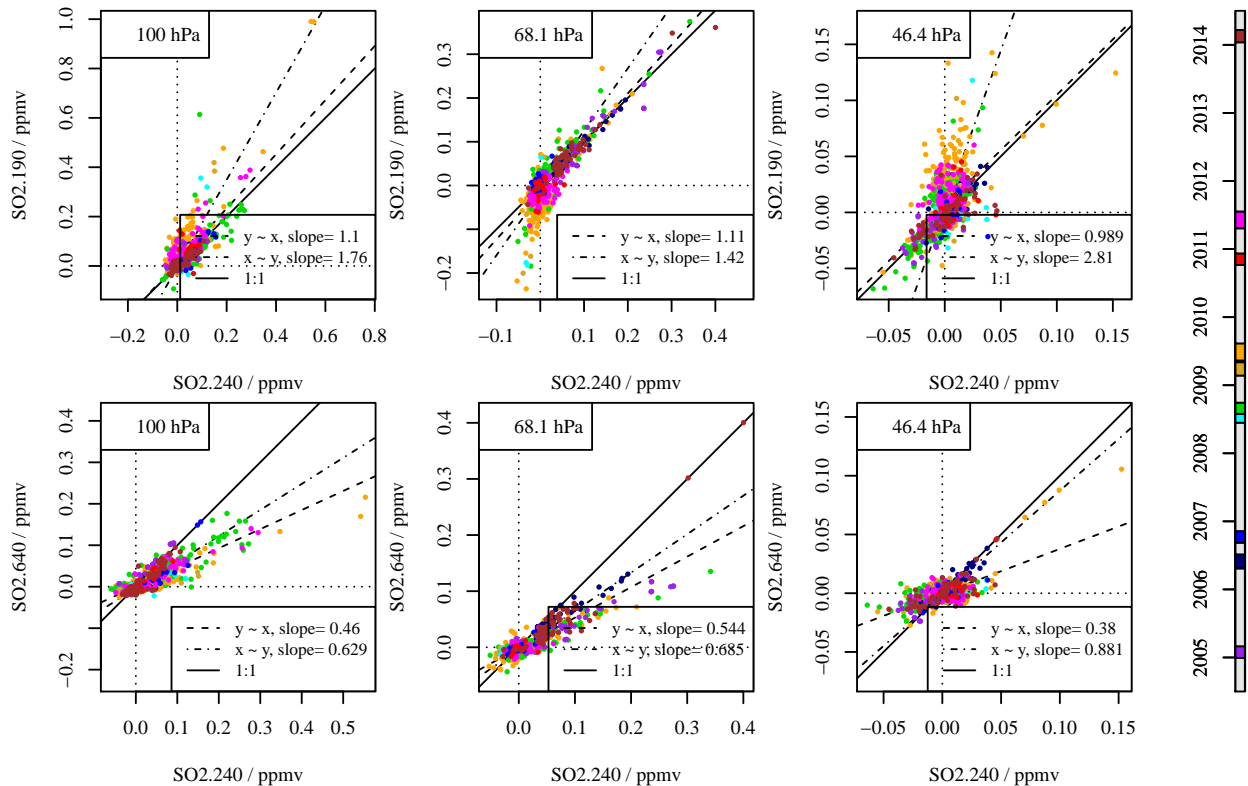


Figure 13. Scatter plots of the 240 GHz SO₂ against the estimates of the same molecule from the 190 (top row) and 640 GHz (bottom row) radiometers. We show only the three pressure levels at which all three radiometers provide usable data. Data are shown only from periods with enhanced volcanic SO₂; a different colour is used for each such period. See Table 1 for details of which volcano was the cause of each period of enhanced SO₂.

6.2 Comparison with OMI

The OMI instrument is described by Levelt et al. (2006). OMI is a nadir UV/visible imaging spectrometer. In its usual operating mode it observes a 2600 km wide swath with 60 image pixels across the width of the swath. The pixels are 24 km across at nadir, becoming wider towards the edges of the swath. In the along-track direction the pixels are 13 km across. The algorithm used to derive total column SO₂ from OMI measurements is described by Yang et al. (2007). It is suitable for most conditions but underestimates the total column where that column is very large. The error can be as large as 70 % for a column of 400 DU dropping to 20 % for a column of 100 DU. The formula used requires that the vertical distribution of SO₂ is specified. The data files contain four separate estimates of column SO₂, each with a different assumption about the vertical profile. The estimates are called PBL, TRL, TRM and STL, corresponding to centre-of-mass altitudes of 0.9, 2.5, 7.5 and 17 km respectively. The README file supplied with the OMI data states that the STL data are to be used when studying explosive volcanic eruptions where the SO₂ is placed in the upper troposphere or lower stratosphere and that differences in actual centre of mass from 17 km produce only small errors. As the useful

SO₂ measurements from MLS are at 10 km or above, we compare them only to the STL product from OMI.

The OMI instrument has been affected by a somewhat mysterious problem known as the “row anomaly”. This anomaly first appears in the data on 25 June 2007 and affects an increasing number of pixels over the subsequent years.

6.2.1 Method

As the MLS data are vertical profiles of mixing ratio and the OMI data are total column amounts, it is necessary to integrate the MLS profiles with respect to a vertical co-ordinate to form a column amount in order to compare the two data sets. The MLS column value will always be a partial column as the instrument can not observe SO₂ at altitudes below the 315 hPa level. The formula used is derived in Appendix A of Livesey and Snyder (2004), assuming that, between the standard MLS pressure levels, the mixing ratio varies linearly in $\log(p)$. The column amount due only to the SO₂ value at the j th pressure level is

$$N_j = \frac{A}{Mg} f_j \left[\frac{\Delta^+ p}{\Delta^+(\log(p))} - \frac{\Delta^- p}{\Delta^-(\log(p))} \right],$$

where p is pressure, A is Avogadro’s number, g is the acceleration due to gravity, M is the average mole mass of air and

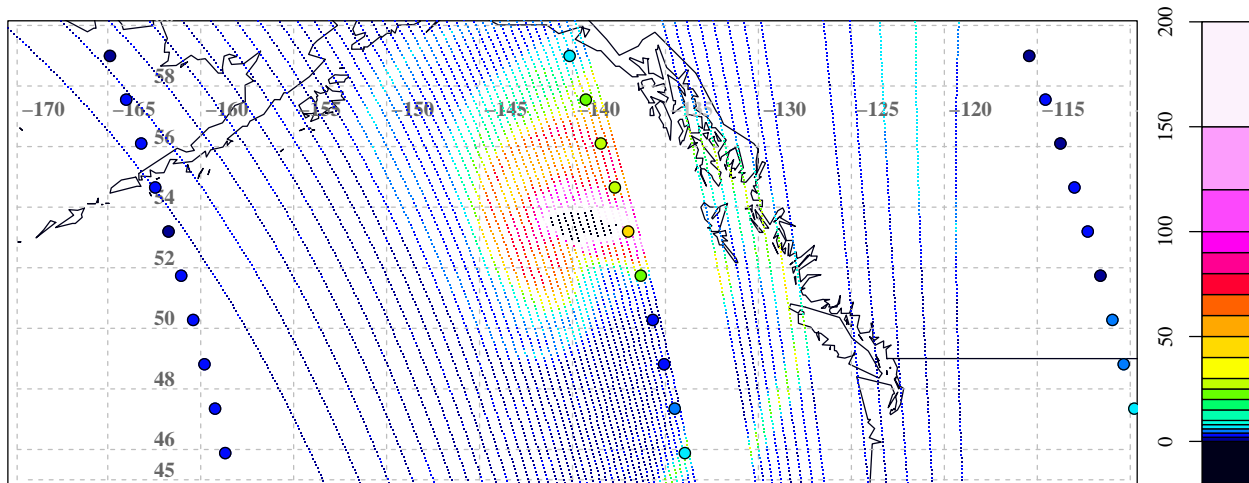


Figure 14. MLS (circles) and OMI (dots) column SO₂ in Dobson units for part of an orbit on 11 August 2008. MLS points are about 160 km apart along the orbit track; two other orbits are shown. OMI pixels are 13 km apart along the orbit track and 24 km apart at nadir across the track. The large gap in the OMI swath to the east of the MLS points is caused by the row anomaly.

f_j is the retrieved volume mixing ratio at the j th pressure level. We use the notation that Δ^+x means the change in x between the j th and the $j+1$ th level; Δ^-x is the change in x between the j th and the $j-1$ th level. The column value for MLS is obtained by summing the N_j values over a suitable range of j . We use SI units for g and p so that we obtain a value of N_j in molecules m^{-2} ; this is then divided by a factor of $2.687 \times 10^{20} m^{-2}$ in order to convert it to Dobson units. If the j th pressure level is the highest pressure level used, the resulting value is essentially an estimate of the column above a pressure halfway in altitude between level j and level $j-1$. The error in the resulting column is a combination of the errors in the mixing ratios at all pressure levels used. As we note in Sect. 2.2, the random errors in the data appear to be larger than the precision estimates supplied with the data. We therefore estimate the error in the MLS partial columns by calculating the standard deviation of the partial columns in a region or day not affected by volcanic SO₂.

The OMI data are provided as column values in Dobson units. As OMI is a nadir sounder and is on the same platform as MLS, its measurement at a given location is made at 425 ± 10 s after the MLS measurement. This 7 min delay is small enough that we do not attempt to correct for it. As the MLS horizontal field of view is narrower than an OMI pixel, we only consider those OMI pixels which are less than 18 km from the line joining successive MLS profile positions. For each MLS profile we form an average of those OMI pixels which meet this criterion and which are closer to that MLS profile than to any other. For most MLS profiles this means that the single MLS column is compared to a mean value of between 12 and 26 OMI pixels. We also calculate the standard deviation of this set of pixels. The slight oblateness of the Earth means that the coincident pixels are not all in the same pixel row of the OMI swath; the coincident row varies

from row 31 (of 60) near the poles to row 39 near the Equator. During the polar summer there may be usable OMI data on the descending half of the orbit; the coincidences for such data may be in a pixel row below the 31st. Figure 14 shows both MLS and OMI column values for a region in the northeast Pacific. Both instruments show a region of large column values; this is due to the eruption of Kasatochi which occurred a few days earlier.

6.2.2 Results

Comparisons as described above can not be performed after January 2009 as the OMI row anomaly affects pixel rows 28–38 from that time onward. We therefore perform such comparisons for periods immediately following the eruptions of Kasatochi on 8 August 2008, Montserrat, on 20 May 2006, Rabaul on 8 October 2006 and Manam on 28 January 2005. The results are shown in Figs. 15 to 18.

The agreement between MLS and OMI is reasonable for Rabaul, Manam and Montserrat, where the SO₂ profile peaks at 68 or 100 hPa. In all three cases, the differences are on the order of 1 DU. This is about 4 times larger than the 0.25 to 0.35 DU variability of the MLS data in the absence of volcanic SO₂, suggesting that a large part of the differences observed is caused by the spatial variability of the volcanic SO₂. For Kasatochi, where there are measurable amounts of SO₂ down to (and presumably below) 315 hPa, the MLS column tends to underestimate the OMI column by many tens of DU, or 100–300%. These differences are very much larger than the 0.8 DU scatter in MLS columns calculated in the same manner in the absence of volcanic SO₂ and are almost certainly due to the presence of SO₂ in the mid-troposphere where OMI is sensitive to it and MLS is not.

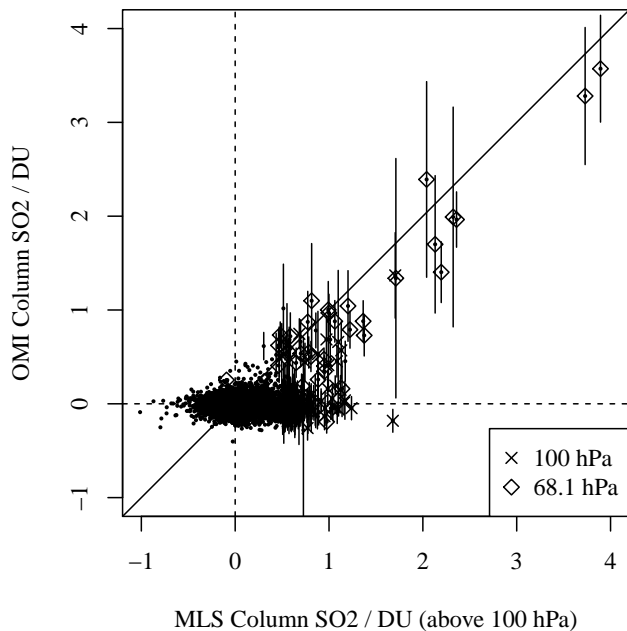


Figure 15. Scatter plot of OMI vs. MLS column SO₂ for the period 20 May 2006 to 9 June 2006 and for the latitude range 9 to 16° N. SO₂ above background levels at this time is attributed to an eruption of the Soufrière Hills volcano in Montserrat. All points are shown by a small dot. Where the MLS SO₂ profile has a clear peak above the background noise, the points are shown with an extra symbol corresponding to the pressure level at which the peak occurs. The error bars represent the standard deviation of the OMI pixels which are averaged to give the values plotted. Note that “above 100 hPa” means that we use the MLS data from this pressure level and levels at higher altitudes. The error in the MLS columns is about 0.25 DU. The solid line shows the ideal 1 : 1 relationship.

6.3 Further validation possibilities

6.3.1 ACE-FTS

The ACE-FTS instrument (Bernath et al., 2005) measures a wide range of chemical species in the upper troposphere and middle atmosphere using the solar occultation technique at visible and near-infrared wavelengths. The technique provides great sensitivity at the cost of limited geographical coverage; data are only available at 15 sunrises and 15 sunsets per day. The latitude at which these events occur changes slowly throughout the year. SO₂ is not a standard ACE-FTS data product, but an experimental SO₂ data set has been produced (Doeringer et al., 2012). We have attempted to compare this data set to the MLS data with no success; the limited coverage of ACE-FTS ensures that on no occasion do the ACE-FTS measurement latitudes coincide with a region of SO₂ which is concentrated enough to be observable by MLS.

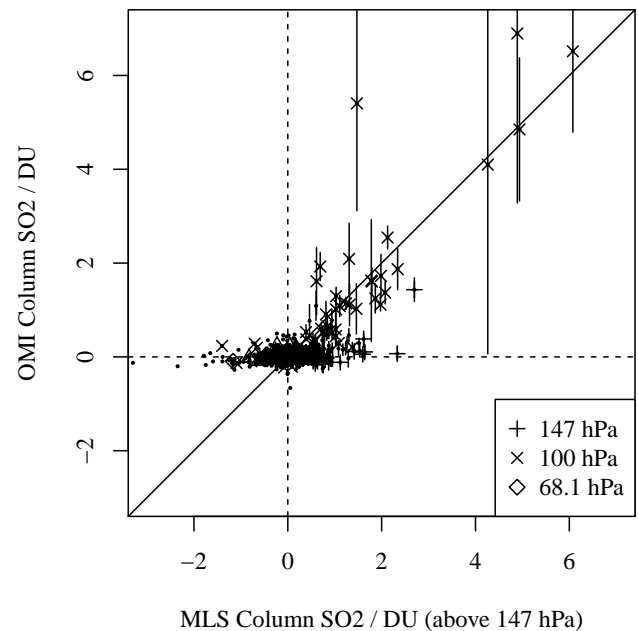


Figure 16. As Fig. 15 but for the period 7–15 October 2006 and for the latitude range 6° S to 8° N. SO₂ above background levels at this time is attributed to an eruption of Rabaul in New Britain, Papua New Guinea. The error in the MLS columns is about 0.35 DU.

6.3.2 MIPAS

MIPAS (Fischer et al., 2008) was an infrared limb-sounding instrument on Envisat. The MIPAS spectrometer was a Fourier transform type, producing spectra with a high spectral resolution. Only a few species were retrieved from these spectra on an operational basis, but experimental retrievals have been produced for a number of other molecules of which SO₂ is one.

Monthly zonal means of SO₂ have been produced by Höpfner et al. (2013). Comparisons of these data to MLS have not proved to be useful as the non-volcanic background in the MLS data is, as we have noted earlier, dominated by systematic errors. The small contribution to the monthly zonal mean from volcanoes affects too small a number of months and latitude bins to provide any kind of useful statistics.

A single-profile retrieval of SO₂ from MIPAS is in development (M. Höpfner, personal communication, 2014). A forthcoming paper (Höpfner et al., 2015) describing that data set will include a comparison with MLS.

6.3.3 IASI

Several recent papers (Clarisse et al., 2012, 2014; Carboni et al., 2012) have demonstrated the potential of the IASI instrument to provide useful SO₂ measurements. In particular, Clarisse et al. (2014) compare the centre of mass of MLS pro-

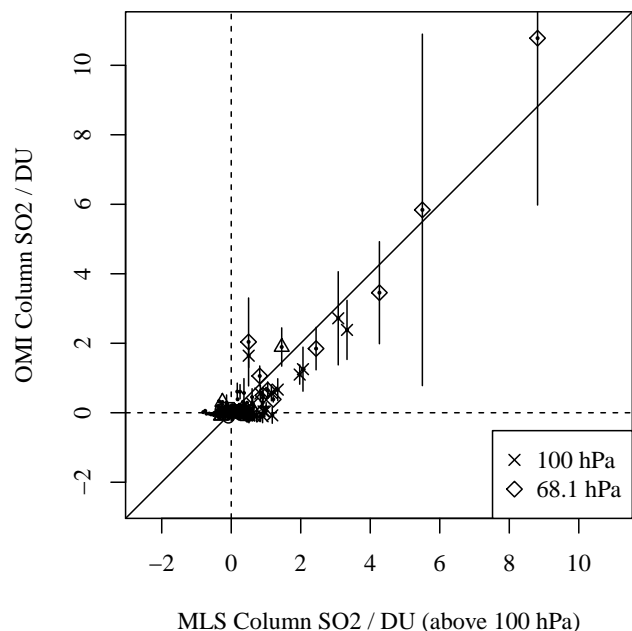


Figure 17. As Fig. 15 but for the period 28–31 January 2005 and for the latitude range 12° S to 7° N. SO₂ above background levels at this time is attributed to an eruption of Manam in Papua New Guinea. The error in the MLS columns is about 0.25 DU.

files with plume heights estimated from IASI and find very good agreement.

7 Discussion

Although the progress we have made in validating the MLS SO₂ data is limited, the results so far are encouraging in that the measurements agree well with OMI, and total masses of SO₂ estimated from the MLS data are in line with values previously published by a variety of authors.

As a tool for studying the dispersion of volcanic SO₂, MLS has both advantages and disadvantages over other currently operating satellite instruments. Its main advantage is that it provides vertical profiles (see Fig. 2) and not just column amounts. The altitude of the SO₂ is therefore measured directly rather than requiring to be inferred from the known meteorology. Its main disadvantage is that the horizontal coverage is very sparse compared to that of most nadir sounders, as shown in Fig. 14. Designs for a future MLS-like instrument (Livesey et al., 2008) provide for viewing directions at a number of angles to the orbit track, allowing for global coverage at a resolution of 50 km; such an instrument would combine the advantages of MLS with those of nadir-sounding instruments and would be particularly valuable for the study of volcanic SO₂.

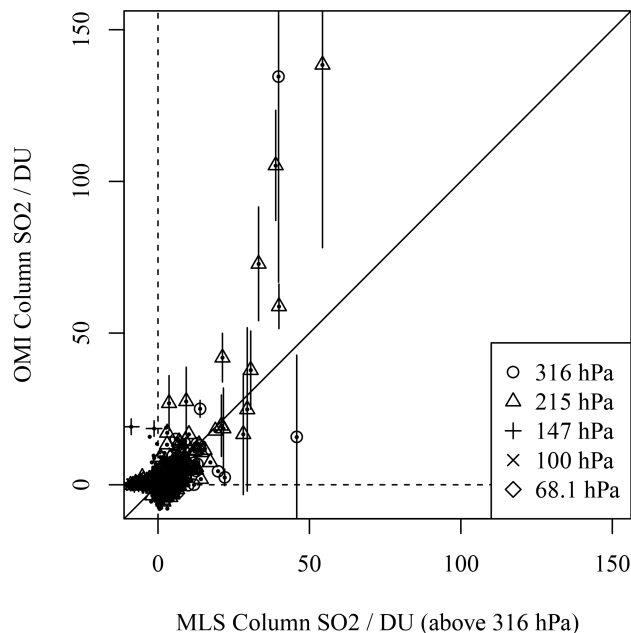


Figure 18. As Fig. 15 but for the period 9–25 August 2008 and for the latitude range 29 to 83° N. SO₂ above background levels at this time is attributed to an eruption of Kasatochi in the Aleutian Islands. The error in the MLS columns is about 0.85 DU.

8 Conclusions

The MLS instrument on Aura has observed enhanced SO₂ mixing ratios following a number of volcanic eruptions of various sizes. Total injected masses of SO₂ calculated from the MLS data agree with previously published values in most cases.

The total column SO₂ calculated from the MLS profiles agrees well with the total column reported by the OMI instrument under the right circumstances. The agreement is good for events where most of the SO₂ is clearly in the stratosphere (Montserrat and Rabaul in 2006, Manam in 2005). Agreement is less good for events where some of the SO₂ is at lower altitudes. This may be because there are significant amounts at altitudes below 215 hPa, where the MLS sensitivity to SO₂ is reduced or zero.

The MLS V2 data show a seasonal cycle with an amplitude of about 2 ppbv which is thought to be spurious. The seasonal effect is smaller than the random error in an individual profile but becomes obvious if sufficient profiles are averaged. This seasonal cycle needs to be removed with some care if calculating the total mass of SO₂ due to a volcanic eruption. Its presence means that the MLS V2 data can not currently be used to study any seasonal cycle which might exist in the non-volcanic SO₂ background.

Acknowledgements. The authors thank Michael Höpfner and Chris Boone for providing preliminary SO₂ retrievals from MIPAS and ACE-FTS for comparison. The authors thank the RCUK open access publication fund for paying publication charges. Work on MLS in the UK has been funded by NERC. MLS data used in this research were produced by the Jet Propulsion Laboratory, California Institute of Technology, under contract with the National Aeronautics and Space Administration.

Edited by: G. Stiller

References

- Bernath, P. F., McElroy, C. T., Abrams, M. C., Boone, C. D., Butler, M., Camy-Peyret, C., Carleer, M., Clerbaux, C., Coheur, P.-F., Colin, R., DeCola, P., DeMaziere, M., Drummond, J. R., Dufour, D., Evans, W. F. J., Fast, H., Fussen, D., Gilbert, K., Jennings, D. E., Llewellyn, E. J., Lowe, R. P., Mahieu, E., McConnell, J. C., McHugh, M., McLeod, S. D., Michaud, R., Midwinter, C., Nassar, R., Nichitiu, F., Nowlan, C., Rinsland, C. P., Rochon, Y. J., Rowlands, N., Semeniuk, K., Simon, P., Skelton, R., Sloan, J. J., Soucy, M.-A., Strong, K., Tremblay, P., Turnbull, D., Walker, K. A., Walkty, I., Wardle, D. A., Wehrle, V., Zander, R., and Zou, J.: Atmospheric Chemistry Experiment (ACE): Mission overview, *Geophys. Res. Lett.*, 32, L15S01, doi:10.1029/2005GL022386, 2005.
- Brühl, C., Lelieveld, J., Crutzen, P. J., and Tost, H.: The role of carbonyl sulphide as a source of stratospheric sulphate aerosol and its impact on climate, *Atmos. Chem. Phys.*, 12, 1239–1253, doi:10.5194/acp-12-1239-2012, 2012.
- Carboni, E., Grainger, R., Walker, J., Dudhia, A., and Siddans, R.: A new scheme for sulphur dioxide retrieval from IASI measurements: application to the Eyjafjallajökull eruption of April and May 2010, *Atmos. Chem. Phys.*, 12, 11417–11434, doi:10.5194/acp-12-11417-2012, 2012.
- Carn, S. A. and Prata, F. J.: Satellite based constraints on explosive SO₂ release from Soufrière Hills Volcano, Montserrat, *Geophys. Res. Lett.*, 37, L00E22, doi:10.1029/2010GL044971, 2010.
- Carn, S. A., Krueger, A. J., Krotkov, N. A., Yang, K., and Evans, K.: Tracking volcanic sulfur dioxide clouds for aviation hazard mitigation, *Nat. Hazards*, 51, 325–343, doi:10.1007/s11069-008-9228-4, 2008.
- Clarisse, L., Hurtmans, D., Clerbaux, C., Hadji-Lazaro, J., Ngadi, Y., and Coheur, P.-F.: Retrieval of sulphur dioxide from the infrared atmospheric sounding interferometer (IASI), *Atmos. Meas. Tech.*, 5, 581–594, doi:10.5194/amt-5-581-2012, 2012.
- Clarisse, L., Coheur, P.-F., Theys, N., Hurtmans, D., and Clerbaux, C.: The 2011 Nabro eruption, a SO₂ plume height analysis using IASI measurements, *Atmos. Chem. Phys.*, 14, 3095–3111, doi:10.5194/acp-14-3095-2014, 2014.
- D'Amours, R., Malo, A., Servranckx, R., Bensimon, D., Trudel, S., and Gauthier-Bilodeau, J.-P.: Application of the atmospheric Lagrangian particle dispersion model MLDP0 to the 2008 eruptions of Okmok and Kasatochi volcanoes, *J. Geophys. Res.*, 115, D00L11, doi:10.1029/2009JD013602, 2010.
- Doeringer, D., Eldering, A., Boone, C. D., González Abad, G., and Bernath, P. F.: Observation of sulfate aerosols and SO₂ from the Sarychev volcanic eruption using data from the Atmospheric Chemistry Experiment (ACE), *J. Geophys. Res.*, 117, D03203, doi:10.1029/2011JD016556, 2012.
- Fischer, H., Birk, M., Blom, C., Carli, B., Carlotti, M., von Clarmann, T., Delbouille, L., Dudhia, A., Ehhalt, D., Endemann, M., Flaud, J. M., Gessner, R., Kleinert, A., Koopman, R., Langen, J., López-Puertas, M., Mosner, P., Nett, H., Oelhaf, H., Perron, G., Remedios, J., Ridolfi, M., Stiller, G., and Zander, R.: MIPAS: an instrument for atmospheric and climate research, *Atmos. Chem. Phys.*, 8, 2151–2188, doi:10.5194/acp-8-2151-2008, 2008.
- Haywood, J. M., Jones, A., Clarisse, L., Bourassa, A., Barnes, J., Telford, P., Bellouin, N., Boucher, O., Agnew, P., Clerbaux, C., Coheur, P., Degenstein, D., and Braesicke, P.: Observations of the eruption of the Sarychev volcano and simulations using the HadGEM2 climate model, *J. Geophys. Res.*, 115, D21212, doi:10.1029/2010JD014447, 2010.
- Höpfner, M., Glatthor, N., Grabowski, U., Kellmann, S., Kiefer, M., Linden, A., Orphal, J., Stiller, G., von Clarmann, T., Funke, B., and Boone, C. D.: Sulfur dioxide (SO₂) as observed by MIPAS/Envisat: temporal development and spatial distribution at 15–45 km altitude, *Atmos. Chem. Phys.*, 13, 10405–10423, doi:10.5194/acp-13-10405-2013, 2013.
- Höpfner, M., Boone, C. D., Funke, B., Glatthor, N., Grabowski, U., Gunther, A., Kellmann, S., Kiefer, M., Linden, A., Pumphrey, H. C., Read, W. G., Roiger, A., Stiller, G., Schlager, H., von Clarmann, T., and Wissmuller, K.: Sulfur dioxide (SO₂) from MIPAS in the upper troposphere and lower stratosphere, *Atmos. Chem. Phys. Discuss.*, in preparation, 2015.
- Krotkov, N. A., Schoeberl, M. R., Morris, G. A., Carn, S., and Yang, K.: Dispersion and lifetime of the SO₂ cloud from the August 2008 Kasatochi eruption, *J. Geophys. Res.*, 115, D00L20, doi:10.1029/2010JD013984, 2010.
- Levelt, P. F., van den Oord, G. H. J., Dobber, M. R., Mälkki, A., Visser, H., de Vries, J., Stammes, P., Lundell, J., and Saari, H.: The Ozone Monitoring Instrument, *IEEE T. Geosci. Remote*, 44, 1093–1101, doi:10.1109/TGRS.2006.872333, 2006.
- Likens, G. E. and Bormann, F. H.: Acid Rain: A Serious Regional Environmental Problem, *Science*, 184, 1176–1179, doi:10.1126/science.184.4142.1176, 1974.
- Livesey, N., Santee, M., Stek, P., Waters, J., Levelt, P., Veefkind, P., Kumer, J., and Roche, A.: A future “Global Atmospheric Composition Mission” (GACM) concept, in: 2008 IEEE Aerospace Conference, IEEE, doi:10.1109/AERO.2008.4526243, 2008.
- Livesey, N. J. and Snyder, W. V.: EOS MLS Retrieval Processes Algorithm Theoretical Basis, Tech. Rep. JPL D-16159, JPL, available at: http://mls.jpl.nasa.gov/data/eos_algorithm_atbd.pdf (last access: 5 January 2015), version 2.0, 2004.
- Livesey, N. J., Snyder, W. V., Read, W. G., and Wagner, P. A.: Retrieval algorithms for the EOS Microwave Limb Sounder (MLS) instrument, *IEEE T. Geosci. Remote*, 44, 1144–1155, 2006.
- Livesey, N. J., Read, W. G., Lambert, A., Cofield, R. E., Cuddy, D. T., Froidevaux, L., Fuller, R. A., Jarnot, R. F., Jiang, J. H., Jiang, Y. B., Knosp, B. W., Kovalenko, L. J., Pickett, H. M., Pumphrey, H. C., Santee, M. L., Schwartz, M. J., Stek, P. C., Wagner, P. A., Waters, J. W., and Wu, D. L.: Earth Observing System (EOS) Aura Microwave Limb Sounder (MLS) Version 2.2 and 2.3 Level 2 data quality and description document, Tech. Rep. JPL D-33509, NASA Jet Propulsion Laboratory California Institute of Technology, Pasadena, California, 91109-8099,

- available at: <http://mhs.jpl.nasa.gov> (last access: 5 January 2015), 2007.
- Loughlin, S. C., Luckett, R., Ryan, G., Christopher, T., Hards, V., Angelis, S. D., Jones, L., and Strutt, M.: An overview of lava dome evolution, dome collapse and cyclicity at Soufrière Hills Volcano, Montserrat, 2005–2007, *Geophys. Res. Lett.*, **37**, L00E16, doi:10.1029/2010GL042547, 2010.
- Matoza, R. S., Pichon, A. L., Vergoz, J., Herry, P., Lalande, J.-M., il Lee, H., Che, I.-Y., and Rybin, A.: Infrasonic observations of the June 2009 Sarychev Peak eruption, Kuril Islands: Implications for infrasonic monitoring of remote explosive volcanism, *J. Volcanol. Geoth. Res.*, **200**, 35–48, 2011.
- Prata, A. J., Carn, S. A., Stohl, A., and Kerkmann, J.: Long range transport and fate of a stratospheric volcanic cloud from Soufrière Hills volcano, Montserrat, *Atmos. Chem. Phys.*, **7**, 5093–5103, doi:10.5194/acp-7-5093-2007, 2007.
- Read, W. G., Froidevaux, L., and Waters, J. W.: Microwave Limb Sounder measurement of stratospheric SO₂ from the Mt. Pinatubo volcano, *Geophys. Res. Lett.*, **20**, 1299–1302, doi:10.1029/93GL00831, 1993.
- Robock, A.: Volcanic eruptions and climate, *Rev. Geophys.*, **38**, 191–219, doi:10.1029/1998RG000054, 2000.
- Robock, A. and Mao, J.: The Volcanic Signal in Surface Temperature Observations, *J. Climate*, **8**, 1086–1103, 1995.
- Rybin, A., Chibisova, M., Webley, P., Steensen, T., Izbekov, P., Neal, C., and Realmuto, V.: Satellite and ground observations of the June 2009 eruption of Sarychev Peak volcano, Matua Island, Central Kuriles, *B. Volcanol.*, **73**, 1377–1392, doi:10.1007/s00445-011-0481-0, 2011.
- Schoeberl, M. R., Douglass, A. R., Hilsenrath, E., Bhartia, P. K., Barnett, J., Beer, R., Waters, J., Gunson, M., Froidevaux, L., Gille, J., Levelt, P. F., and DeCola, P.: Overview of the EOS Aura Mission, *IEEE T. Geosci. Remote*, **44**, 1066–1074, 2006.
- Wadge, G., Robertson, R., and Voight, B.: Eruption of Soufrière Hills Volcano, Montserrat from 2000 to 2010, in: *Eruption of Soufrière Hills Volcano, Montserrat from 2000 to 2010*, edited by: Wadge, G., Robertson, R. E. A., and Voight, B., Vol. 39 of *Geological Society Memoirs*, 1–501, doi:10.1144/M39.0, 2014.
- Waters, J. W., Froidevaux, L., Harwood, R., Jarnot, R., Pickett, H., Read, W., Siegel, P., Cofield, R., Filipiak, M., Flower, D., Holden, J., Lau, G., Livesey, N., Manney, G., Pumphrey, H., Santee, M., Wu, D., Cuddy, D., Lay, R., Loo, M., Perun, V., Schwartz, M., Stek, P., Thurstans, R., Boyles, M., Chandra, S., Chavez, M., Chen, G.-S., Chudasama, B., Dodge, R., Fuller, R., Girard, M., Jiang, J., Jiang, Y., Knosp, B., LaBelle, R., Lam, J., Lee, K., Miller, D., Oswald, J., Patel, N., Pukala, D., Quintero, O., Scaff, D., Snyder, W., Tope, M., Wagner, P., and Walch, M.: The Earth Observing System Microwave Limb Sounder (EOS MLS) on the Aura satellite, *IEEE T. Geoscience Remote*, **44**, 1106–1121, 2006.
- Waythomas, C. F., Scott, W. E., Prejean, S. G., Schneider, D. J., Izbekov, P., and Nye, C. J.: The 7–8 August 2008 eruption of Kasatochi Volcano, central Aleutian Islands, Alaska, *J. Geophys. Res.*, **115**, B00B06, doi:10.1029/2010JB007437, 2010.
- Yang, K., Krotkov, N. A., Krueger, A. J., Carn, S. A., Bhartia, P. K., and Levelt, P. F.: Retrieval of large volcanic SO₂ columns from the Aura Ozone Monitoring Instrument: Comparison and limitations, *J. Geophys. Res.*, **112**, D24S43, doi:10.1029/2007JD008825, 2007.
- Yang, K., Liu, X., Bhartia, P. K., Krotkov, N. A., Carn, S. A., Hughes, E. J., Krueger, A. J., Spurr, R. J. D., and Trahan, S. G.: Direct retrieval of sulfur dioxide amount and altitude from spaceborne hyperspectral UV measurements: Theory and application, *J. Geophys. Res.*, **115**, D00L09, doi:10.1029/2010JD013982, 2010.